RSC Advances

PAPER

Cite this: *RSC Adv.*, 2023, **13**, 2552

A bis-chalcone based colorimetric probe for the selective detection of bisulfite/sulfite anions: exploring surfactant promoted Michael addition of anions to α, β-unsaturated ketones†

Sowmya P, Sivakrishna Prakash and Abraham Joseph *

Received 29th October 2022
Accepted 1st January 2023

DOI: 10.1039/d2ra06832j

rsc.li/rsc-advances

A probe, (1E,4E)-1,5-di(thiophen-2-yl)penta-1,4-dien-3-one, was developed for rapid, colorimetric, and selective detection of bisulfite/sulfite anions in aqueous solutions. This probe is based on the Michael addition reaction which is favoured in the presence of cationic micellar medium CTAB. CTAB promoted Michael addition is an effective tool to determine SO_2 toxicity, which is mainly expressed in terms of collective concentration of bisulfite and sulfite anions. The probe showed high selectivity and sensitivity toward bisulfite and sulfite over other interfering anions, with a detection limit of 0.43 μM and 0.23 μM, respectively. The possible recognition mechanism of the probe and the analyte was illustrated by NMR, HR-MS, IR, and computational analysis. Moreover, this probe showed great potential for the detection of bisulfite/sulfite in real samples, such as crystal sugar and brown sugar.

1. Introduction

Sulfur dioxide (SO_2) is a well-known air pollutant released in many industrial processes and it exhibits significant impacts on human health and the environment.[1,2] Studies have shown that frequent exposure to SO_2 induces many health issues such as lung and brain cancer, cardiovascular diseases, respiratory problems, and neurological disorders.[3–6] Since SO_2 can be easily hydrated to sulfurous acid once inhaled and subsequently forms an equilibrium state between its derivatives bisulfite (HSO_3^-) and sulfite (SO_3^{2-}) as its main forms in aqueous media, so the toxicity of SO_2 is determined mainly by these two anions.[7]

Sulfur dioxide (SO_2) derivatives such as sulfite and bisulfite anions have been widely used as preservatives and additives in many food items, beverages, and pharmaceutical products to preserve freshness and increase their shelf life.[8] However, excessive intake of bisulfites/sulfites would induce adverse effects on human health.[9] Hence, the sulfite intake by the human body must be limited. This demands the development of rapid, selective, and sensitive methods for the detection and quantification of SO_2 derivatives.

To date, the existing conventional methods to detect bisulfite/sulfites include ion chromatography,[10,11] spectroscopy,[12–15] electrochemistry,[16,17] and iodometric titration.[18] However, the main disadvantage of these methods is that the majority of them require miscellaneous sample pre-treatment and the use of relatively multiple reagents. Among these conventional approaches, spectroscopy has been widely applied in analyte detection because of its high selectivity, simplicity, low detection limit, and suitability for real-time monitoring. Therefore, calorimetric and fluorescent probes have been regarded as versatile tools for monitoring ions and biomolecules.[19–22]

Till now, several colorimetric and fluorescent probes for the detection of the SO_2 derivatives (HSO_3^-/SO_3^{2-}) have been designed and developed based on different sensing mechanisms such as the selective deprotection of levulinate group,[23–25] complexation with amines,[26,27] the selective reaction with aldehyde,[28,29] coordination to metal ions,[30] and Michael-type additions.[31,32] Among these different approaches 1,4–Michael addition of nucleophiles to α, β unsaturated systems that contain ester, ketone, nitrile, and nitro groups is one of the most versatile methods[33,34] for the development of chemosensors for the detection of SO_2 derivatives because this method allows the reaction to proceed under mild conditions.[35–39]

Interestingly, Zhang *et al.* (2013)[38] reported promising studies in this area, using a cationic cetyltrimethylammonium bromide (CTAB) micelle, to create a hydrophobic and basic microenvironment that promotes the addition reaction of sulfite to an activated olefin in aqueous solutions. The limit of detection of the probe was 0.2 μM. Based on this study, many groups have reported new probes that can detect SO_2 derivatives in aqueous solutions *via* micelle-mediated Michael-type addition reaction. In 2017, Gómez *et al.* reported two fluorescent turn-off probes for the detection of SO_2 derivatives in a micellar

Department of Chemistry, University of Calicut, Calicut University, 673 635, Kerala, India. E-mail: abrahamjoseph@uoc.ac.in

† Electronic supplementary information (ESI) available. See DOI: https://doi.org/10.1039/d2ra06832j

media with a limit of detection in the range of 1–10 μM.[40] Later the same group reported a new chalcocoumarin derivative with an improved LOD of 0.24 μM.[41]

These reports encouraged us to develop a colorimetric probe that shows a rapid, highly selective, and sensitive sensing process for HSO_3^-/SO_3^{2-} in an aqueous solution under mild conditions. Even though the NLO properties and medicinal properties of the developed probe have been explored by many groups, to the best of our knowledge, the sensing property of the probe is explored for the first time. We selected this probe particularly to illustrate the advantage of surfactant promoted Michael addition over simple Michael addition because the surfactant promoted addition allows the sensing of both of the SO_2 derivatives (HSO_3^- and SO_3^{2-}) rather than a single SO_2 derivative (either HSO_3^- or SO_3^{2-}) which allows the accurate determination of SO_2 toxicity. Moreover, this developed probe is promising for the detection of bisulfite/sulfite found in food samples.

2. Experimental

2.1. Reagents, materials, and apparatus

All chemicals and solvents used for synthesis and sensing were purchased from commercial suppliers and used without further purification. IR spectra were performed with a Jasco-FT/IR-4100 spectrophotometer and UV-vis spectra were measured by using a Jasco V-750 spectrophotometer. ^{1}H NMR (400 MHz) and ^{13}C NMR (400 MHz) spectra were recorded on a Bruker AVANCE III-400 MHz NMR spectrometer, and HR-MS data were obtained with a Q-TOF MS spectrometer. The pH measurements were done on a Mettler Toledo pH meter.

2.2. Synthesis of the probe (1E,4E)-1,5-di(thiophen-2-yl) penta-1,4-dien-3-one

(1E,4E)-1,5-di-2-thienylpenta-1,4-dien-3-one (probe) was synthesized by Claisen–Schmidt reaction (Scheme 1) and characterized using FT-IR, ^{1}H NMR, ^{13}C NMR, and Mass spectroscopic techniques. A modified procedure used for the synthesis[42] and characterization is given in the ESI data.†

2.3. Sample preparation, methods, and measurements

2.3.1. Absorbance titration. An accurately weighed amount of buffering agent was added to ultra-pure water to make a HEPES buffer solution (20 mM, pH 7.4) and an accurately weighed amount of the probe was dissolved in DMF to obtain a 1 $\times$ 10^{-3} M probe stock solution. All other solutions employed in this study were prepared in HEPES buffer. Stock solutions of surfactant CTAB (10^{-1} M) and probe were added to 3 mL of the HEPES buffer solution taken in the cuvette to make [CTAB] = 1 mM and [probe] = 1 $\times$ 10^{-5} M. 0–12 μL of 10 mM of analyte ($NaHSO_3$/Na_2SO_3)-buffer stock solution was added into the cuvette containing probe-surfactant buffer solution. Absorption spectra were measured with a Jasco V-750 UV-visible spectrophotometer.

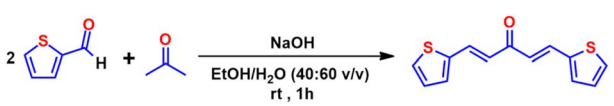

Scheme 1 The synthesis procedure of the probe.

2.3.2. pH titrations. The pH of probe-surfactant solutions was adjusted with HCl or NaOH aqueous solution and absorption spectra were recorded after the addition of a fixed amount (20 eq.) of analyte solution.

2.3.3. Detection limit. The absorption intensity of the probe with $NaHSO_3$ and Na_2SO_3 has measured three times and the standard deviation of the calibration curve was determined. The detection limit (LOD) was obtained by $3\sigma/k$, where σ is the standard deviation of the calibration curve, and k is the slope of the plot of absorption intensity *versus* sample concentration.

2.3.4. Reproducibility. The stability of the method was investigated by calculating the Relative Standard Deviation (RSD) of three absorbance measurements in the presence of the analyte after 7 minutes.

2.3.5. Selectivity and competition study. All the testing anions (F^-, Cl^-, Br^-, I^-, AcO^-, HCO_3^-, CO_3^{2-}, HPO_4^{2-}, SO_4^{2-}, NO_3^-, $S_2O_3^{2-}$, CN^-, SCN^-) were prepared from their sodium salts. The solutions of cysteine (Cys.) were prepared in redistilled water. A selectivity study was conducted by adding 20 eq. of interfering ions to a 10 μM probe solution, and a competition study was conducted by adding 10 eq. of HSO_3^-/SO_3^{2-} to a 10 μM probe solution in the presence of 20 eq. of interfering ions.

2.4. Measurement of spiked sulfite in realistic samples

Crystal sugar and brown sugar were purchased from a supermarket and were used without further pre-treatment. Sugar sample solutions were prepared by dissolving 25 g of sugar in deionized water and diluting it to 100 mL. Stock solutions of CTAB, probe and a known volume of sugar sample solution were added to 3 mL of the buffer solution to make [CTAB] = 1 mM and [probe] = 1 $\times$ 10^{-5} M, and after 7 min, the absorption intensities were recorded. Sugar samples were then spiked with different concentrations of $NaHSO_3$ (5.10 μM) and Na_2SO_3 (5.10 μM) that had been accurately prepared. The resulting samples were then treated with the probe for 7 min and the absorption intensities were recorded. The concentration of the sample was determined using a calibration plot.

3. Results and discussion

Fig. 1 shows the time-dependent absorbance of the probe in the presence of bisulfite/sulfite in HEPES buffer (20 mM, pH 7.4) containing 1 mM CTAB. As the reaction progressed, the absorption peak centered at 383 nm decreased, along with the simultaneous emergence of a new absorption at 328 nm; after that, the absorption at 328 nm gradually increased first and then decreased accompanied by the solution color changing from yellow to colourless (inset in Fig. 1). The isosbestic point (337 nm) indicates a clear formation of a new compound and decrease in the peak at 328 nm may be due to the decomposition or aggregation of product molecules. The probe was

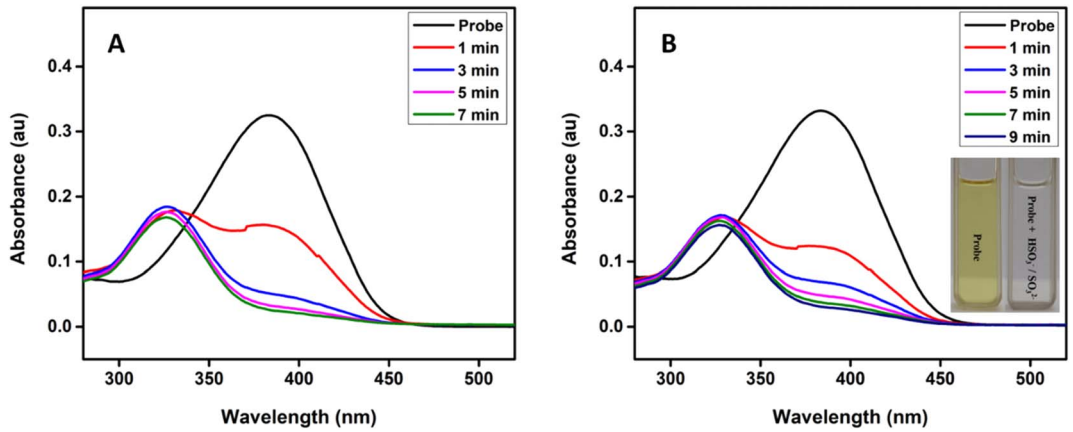

Fig. 1 (A) Time-dependent absorption of the probe (10 μM) in the presence of 20 eq. of bisulfite and (B) sulfite respectively in CTAB–HEPES (1 mM) system. The insets show the visible color change of the probe with 20 eq. of bisulfite/sulfite for 10 minutes in CTAB–HEPES system (20 mM HEPES, pH 7.4) at 25 °C.

transformed to the addition product by 5 min and 7 min after the addition of HSO_3^- and SO_3^{2-} respectively. Therefore, the assay time of 7 min was used in the evaluation of the selectivity and sensitivity of the probe toward the analytes.

To investigate the spectral changes of the probe toward HSO_3^- and SO_3^{2-}, the absorption titration was performed at optimal experimental conditions. Fig. 2 shows the spectral behaviour upon the addition of HSO_3^- and SO_3^{2-} to the probe solution, which indicates a behaviour similar to that of a time-dependent study. A notable color change with increasing the concentration of the analyte was observed, suggesting that the present probe could serve as a colorimetric probe for the detection of SO_2 derivatives.

The marked blue shifts in the absorbance spectra could be attributed to the Michael addition of bisulfite/sulfite to the electrophilic C=C double bond in the probe, leading to a non-conjugated structure of the reaction product. To confirm the formation of the addition product probe-SO_3H, the probe was treated with Na_2SO_3, and the reaction product was isolated.

To provide evidence for the sensing mechanism, ^{1}H NMR,^{13}C NMR, HR-MS, and IR analysis of the probe and its reaction product with HSO_3^-/SO_3^{2-} (probe-SO_3H) were performed. Surprisingly, the result from the HRMS-ESI (Fig. 3) shows a major ion peak at $m/z = 359.2409$ which is identical to the theoretical molecular mass of the probe-OH adduct ([probe-2OH 2K]$^{2+}$ calcd = 359.97) rather than probe-SO_3H adduct. The proposed mechanism of formation of the probe-OH adduct is shown in Scheme 2. These data strongly support the 1 : 2 adduct (probe-SO_3H adduct) formation of the probe with HSO_3^-/SO_3^{2-} which undergoes an elimination reaction to form probe-OH adduct as the final product.

Furthermore, the formation of the adduct was also confirmed by ^{13}C NMR (Fig. S1†), DEPT (Fig. S2†) and ^{1}H NMR (Fig. S3† and Fig. S4†) analysis. As shown in Fig. S5,† the resonance signal corresponding to the alkene proton H_β at 7.8 ppm (d) of the probe disappeared, and a new peak at 4.71 ppm (dd) emerged from the protons at C_β carbon of the probe-OH adduct, which confirms the addition of bisulfite/sulfite to C=C group. Also, the addition of bisulfite/sulfite to C=C resulted in the formation of a chiral center at C_β of the probe-OH adduct, and as the result, the two protons of the methylene group at C_α of the probe-OH adduct were found to be

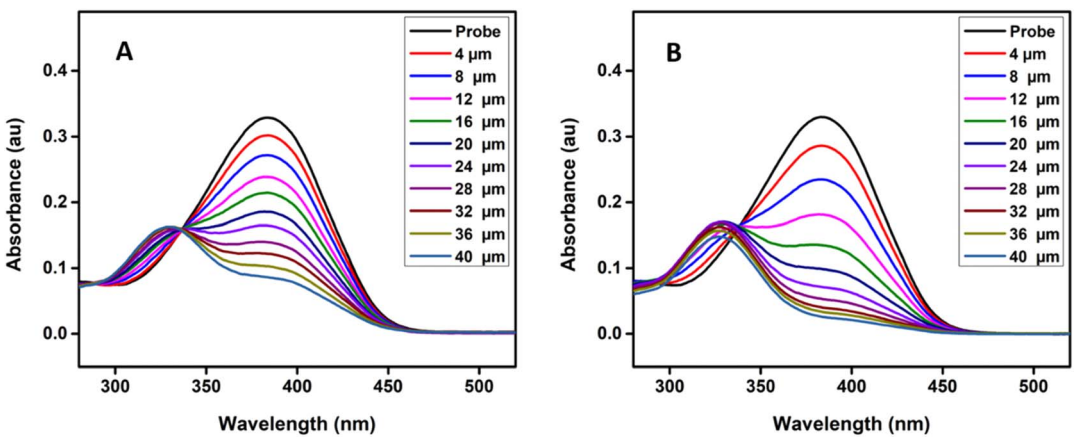

Fig. 2 (A) Absorption spectra of probe (10 μM) upon the addition of increasing concentration of $NaHSO_3$ and (B) Na_2SO_3 respectively from 0 to 40 μM in HEPES buffer solution (20 mM, pH 7.4) at 25 °C.

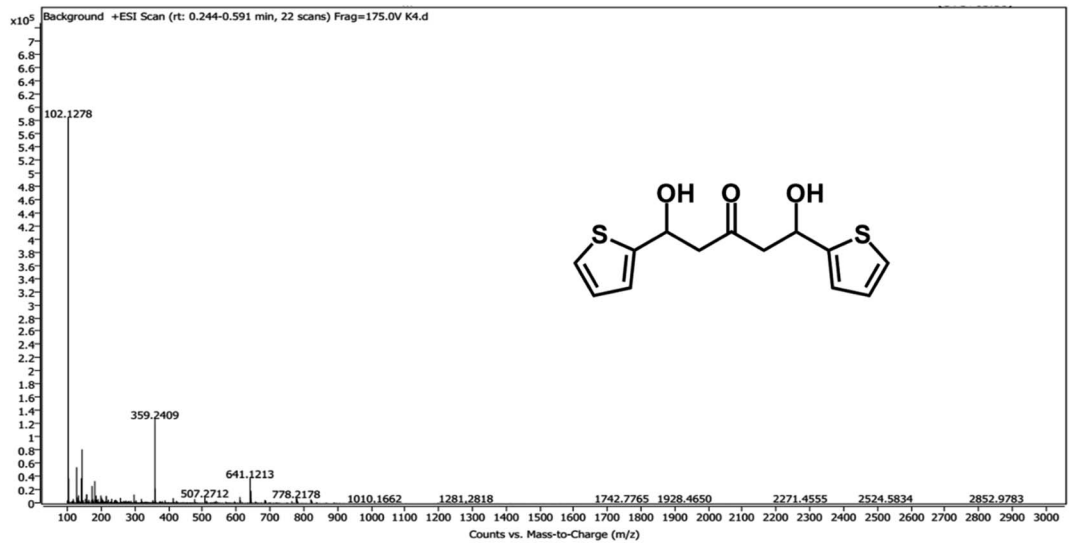

Fig. 3 HRMS-ESI of the adduct (probe-OH) formed by the reaction between the probe and HSO_3^-/SO_3^{2-}.

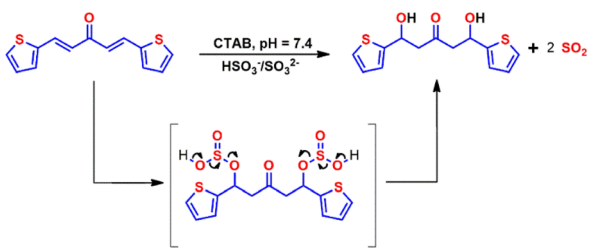

Scheme 2 The proposed mechanism of the probe for SO_2 derivatives HSO_3^-/SO_3^{2-}.

non-equivalent. Therefore, the signal for H_α of the probe at 6.8 ppm (d) shifted to a higher field in the probe-OH adduct and appeared as two doublets of a doublet in the range of 3.15–3.51 ppm. ^{13}C resonance peaks of C_α and C_β (Fig. S6†) show a shift from 135.6 and 128.8 ppm to 46 and 56.6 ppm respectively on moving from the probe to probe-OH adduct, which also confirms the addition of bisulfite/sulfite to the double bond to form a Michael adduct.

IR spectra of the probe (Fig. S7†) show two characteristic peaks at 1604 cm^{-1} and 1661 cm^{-1} which correspond to the C=C group and C=O group respectively. In the case of probe-OH, the peak at 1604 cm^{-1} disappeared and a new peak appeared at 2972 cm^{-1} (C–H stretching of alkane) due to the addition of HSO_3^-/SO_3^{2-} to the C=C group during the step leading to the formation of final product probe-OH adduct. On the other hand, the carbonyl peak at 1661 cm^{-1} was shifted to 1650 cm^{-1} may be due to the formation of a hydrogen bond with the –OH group of the probe-OH adduct. IR spectra of the probe-OH show two more new peaks around 3394 (broad) and 1402 cm^{-1} which corresponds to O–H stretching of alcohol and O–H bending of alcohol respectively. This result is consistent with the addition of HSO_3^-/SO_3^{2-} to the C=C group and the formation of the probe-OH adduct from the probe-SO_3H adduct.

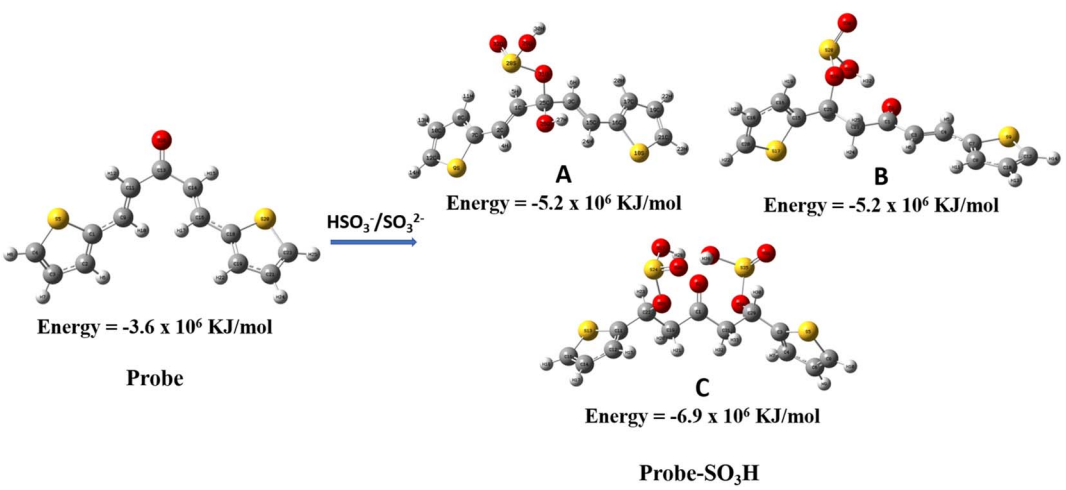

Fig. 4 The optimized structures of the probe and its expected reaction products (probe-SO_3H) of reaction with HSO_3^-/SO_3^{2-}.

To confirm the proposed sensing mechanism of HSO_3^-/SO_3^{2-} by the probe, the density functional theory (DFT) was carried out at the B3LYP/6-311+G(d,p) level by the Gaussian 09 program.

The optimized structures in the ground states of the probe and possible products of the reaction between the probe and SO_2 derivatives were shown in Fig. 4. *A* represents the product formed by the 1,2 addition of SO_2 derivatives to the probe, and *B* represents the product formed by the 1,4 addition of SO_2 derivatives to the probe at only one olefinic site. The stabilization energy of *A* and *B* differ slightly but are almost the same as -5.2×10^6 KJ mol^{-1}. *C* represents the product formed by the 1,4 addition of SO_2 derivatives to the probe at both olefinic sites. We found that the stabilization energy of *C* (-6.9×10^6 KJ mol^{-1}) was higher than that of *A* (-5.2×10^6 KJ mol^{-1}), *B* (-5.2×10^6 KJ mol^{-1}), and the probe (-3.6×10^6 KJ mol^{-1}). Since *C* is the more stable product, these results confirm that the Michael addition of HSO_3^-/SO_3^{2-} to the probe takes place at both olefinic sites of the probe. This result was consistent with the experimental results.

Normally, the addition of bisulfite/sulfite to olefin takes place in organic solvents at elevated temperatures or in the presence of catalysts. Here we report the addition of sulfite to olefin under aqueous conditions. To further investigate the reaction mechanism, we also studied the spectral response of the probe toward bisulfite/sulfite in HEPES buffer solution (20 mM, pH 7.4) in the presence and absence of CTAB. No new absorption peak was found even after 1 h in the absence of CTAB (Fig. S8†), which implies that the addition reaction between bisulfite/sulfite and probe cannot occur without CTAB. The slight decrease in the absorbance at 383 nm might be caused by the aggregation or precipitation of probe molecules.

3.1. Effect of pH on the absorbance of the probe towards SO_2-derivatives

To investigate the effect of pH on the absorbance of the probe, the reaction was executed at different pH by adjusting the pH by HCl and NaOH. As shown in Fig. S9† and 5, the absorbance of the probe was almost pH insensitive, whereas upon the interaction with $NaHSO_3$ and Na_2SO_3 important changes were observed depending on the pH values. The reaction proceeds slowly when the solution's pH was less than 6, but it was greatly speeded up when the pH was near and above 7, which shows that a basic environment is essential for this reaction. This behaviour allows the detection of bisulfite/sulfite in physiological conditions; hence we choose a pH of 7.4 for our study.

3.2. Effect of various surfactants on the absorbance of the probe towards SO_2-derivatives

To investigate the effect of various surfactants on the absorbance of the probe, the study was conducted using cationic, anionic, and zwitterionic surfactants. Surfactants affect the chemical reaction in the following ways: changing the local concentrations of the reactants, altering the local pH value, and providing a nonpolar microenvironment.[43,44] Cationic surfactant CTAB can adsorb counter ions such as OH^-, HSO_3^-, SO_3^{2-} *etc*, so the pH value, as well as bisulfite/sulfite concentration, should be much higher on the CTAB micelle surface than in the bulk solution. Therefore, the reaction was accelerated greatly in CTAB–HEPES because the CTAB micelle offered a basic and nonpolar microenvironment. The anionic surfactant sodium dodecylbenzene sulfate (SDBS) also can provide a nonpolar microenvironment, but it adsorbs positively charged ions, as a result, the H^+ concentration around SDBS micelle is higher than that of the bulk solution, this is why the reaction conducted in SDBS-HEPES shows no significant change in the absorption even after 1 h (Fig. S10†). The presence of zwitter ionic surfactant cocamidopropyl betaine (CAPB) also didn't bring any change in absorption spectra after 1 h (Fig. S11†), which suggests that the zwitterionic micelle (CAPB) is less effective than the cationic micelle (CTAB) in binding hydrophilic ions such as SO_2 derivatives.[45] This behaviour of the probe verifies that the charge characteristic of the surfactant plays an essential role in this reaction.

The detection limit (LOD) of the probe for bisulfite/sulfite detection was determined from a plot of absorption intensity as a function of $NaHSO_3$/Na_2SO_3 concentration, as previously mentioned in the experimental section. A good linear

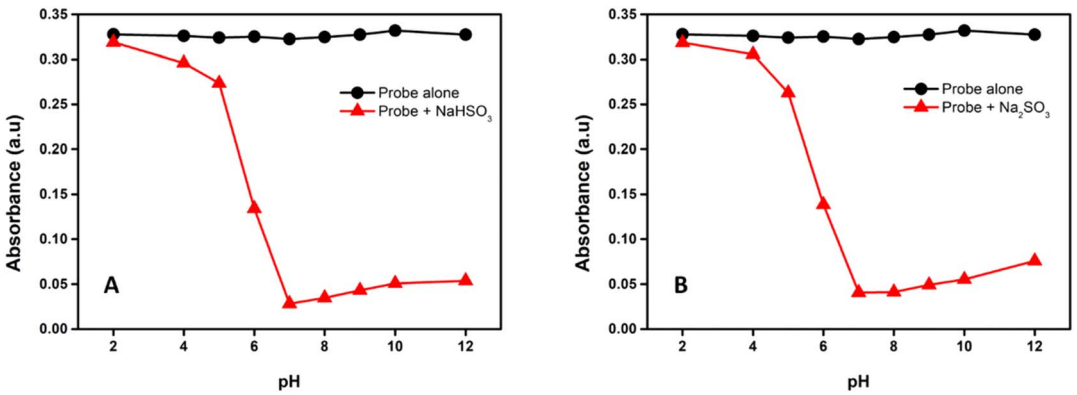

Fig. 5 Effect of pH on the absorbance of the probe (10 μM) alone and after its reaction with (A) $NaHSO_3$ (200 μM) and (B) Na_2SO_3 (200 μM) respectively at 25 °C after 10 minutes of reaction. Absorbance at 383 nm is recorded.

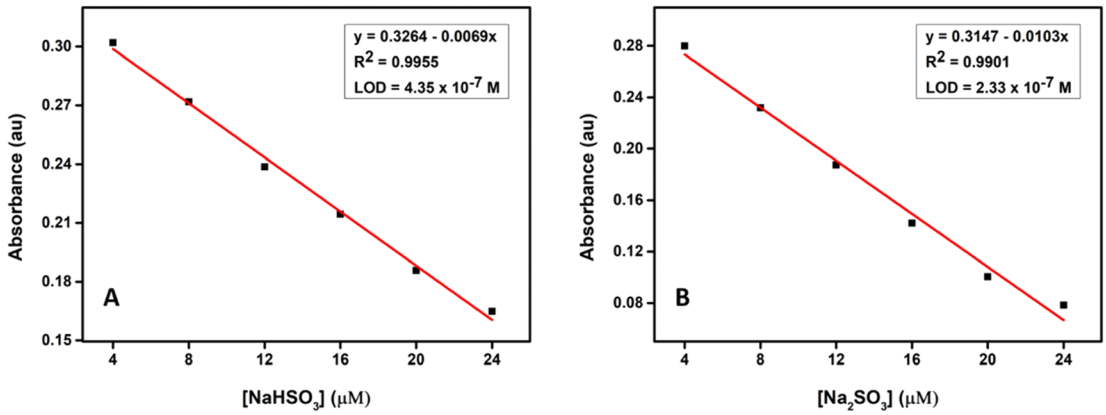

Fig. 6 (A) Changes in absorbance at 383 nm upon the gradual addition of $NaHSO_3$ and (B) Na_2SO_3 respectively in CTAB–HEPES buffer solution (20 mM, pH 7.4) from 4 to 24 μM.

relationship is observed for the probe with a correlation coefficient as large as 0.9955 and 0.9901, and LOD of 0.43 μM and 0.23 μM for the detection of bisulfite (Fig. 6 (A)) and sulfite (Fig. 6 (B)) respectively.

The stability of the method was assessed as mentioned in the experimental section. The relative standard deviation (RSD) associated with the probe was found to be 2.6% and 3.6% for the detection of bisulfite and sulfite respectively, which is <5% showing an acceptable performance and good stability of the method.

3.3. Selectivity and competition of the probe toward SO_2-derivatives

The selectivity of the probe toward SO_2 derivatives over some interfering anions including F^-, Cl^-, Br^-, I^-, AcO^-, HCO_3^-, CO_3^{2-}, HPO_4^{2-}, SO_4^{2-}, NO_3^-, $S_2O_3^{2-}$, CN^-, SCN^-, and biothiol (cysteine) in CTAB–HEPES system was evaluated. As illustrated in Fig. 7, there is no obvious spectral change associated with the probe even in the presence of 20 eq. of most of the interfering anions, which verifies that the probe is highly selective toward bisulfite/sulfite.

Furthermore, competitive analysis of the different interfering anions with HSO_3^-/SO_3^{2-} was conducted, where the interfering anions were first introduced into the probe solution and followed by the addition of 10 eq. of HSO_3^- or SO_3^{2-}. Fig. 8 shows that there is no much change in the absorbance of the probe at 383 nm upon the addition of 20 eq. of different interfering anions, while there is a considerable change in the absorbance during the addition of bisulfite/sulfite to this test solution. This shows that all the tested anions have no interference with the absorbance response of the probe toward HSO_3^-/SO_3^{2-}, thereby indicating its high level of selectivity.

3.4. Detection of SO_2 derivatives in real samples

To demonstrate the applicability of the tested probe, the compound was assessed to detect bisulfite/sulfite in realistic samples. The crystal sugar and brown sugar were purchased from a supermarket and were dissolved and diluted in water as

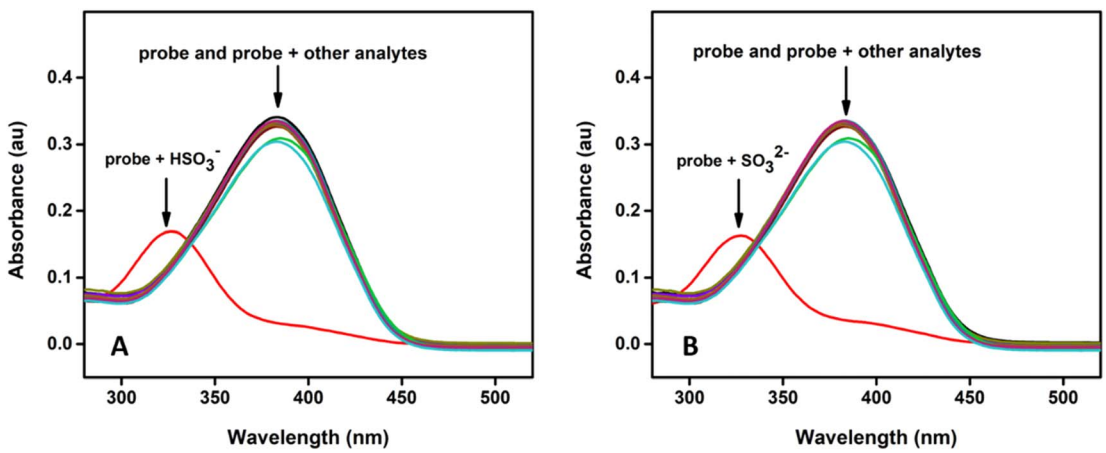

Fig. 7 (A) Absorption changes of probe (10 μM) in the presence of HSO_3^- (100 μM), (B) SO_3^{2-} (100 μM), and various other analytes (200 μM). Other analytes are: F^-, Cl^-, Br^-, I^-, AcO^-, HCO_3^-, CO_3^{2-}, HPO_4^{2-}, SO_4^{2-}, NO_3^-, $S_2O_3^{2-}$, CN^-, SCN^-, and biothiol (cysteine) respectively. All experiments were performed in HEPES buffer (20 mM, pH 7.4) at 25 °C and each spectrum was obtained 7 min after the addition of analyte.

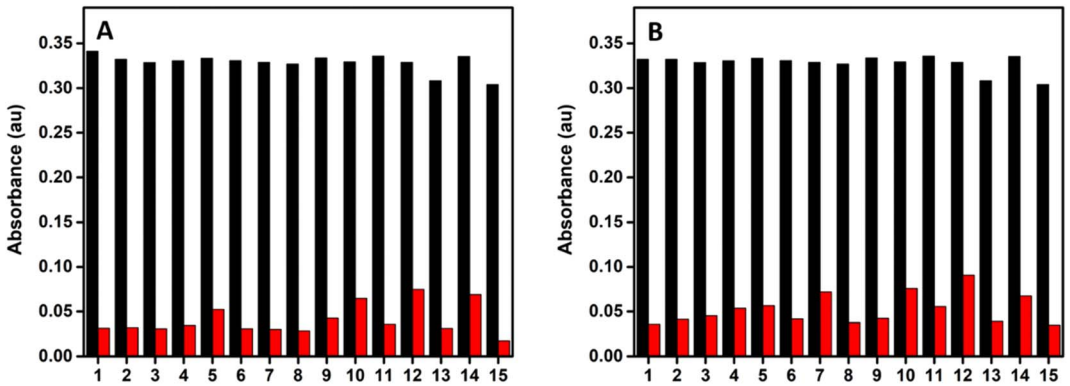

Fig. 8 (A) Absorbance of the probe (10 μM) in the presence of 20 eq. of various additives with (red) or without (black) HSO_3^- (100 μM) and (B) SO_3^{2-} (100 μM) in CTAB–HEPES for 7 minutes: (1) blank; (2) F^-; (3) Cl^-; (4) Br^-; (5) I^-; (6) AcO^-; (7) HCO_3^-; (8) CO_3^{2-}; (9) HPO_4^{2-}; (10) SO_4^{2-}; (11) NO_3^-; (12) $S_2O_3^{2-}$; (13) CN^-; (14) SCN^-; and (15) cysteine.

Table 1 Determination of bisulfite/sulfite in realistic samples[a]

Sample	Present concentration of SO_2 derivatives (μM)	Added HSO_3^- (μM)	Found HSO_3^- (μM)	Recovery (%)	RSD (%)
Crystal sugar	2.19	5	7.38	102.6	1.7
		10	11.95	98.0	5.0
Brown sugar	3.41	5	8.49	100.9	2.2
		10	13.07	97.5	1.3
Sample	Present concentration of SO_2 derivatives (μM)	Added SO_3^{2-} (μM)	Found SO_3^{2-} (μM)	Recovery (%)	RSD (%)
Crystal sugar	2.13	5	7.07	99.2	2.4
		10	11.81	97.4	1.7
Brown sugar	3.39	5	8.63	102.9	2.3
		10	13.93	104.0	1.3

[a] In the sample solution, the concentration of sugar was 25 g/100 mL. Sulfite was spiked to the samples directly and calculated as SO_2. Relative standard deviations were calculated based on three measurements.

the real food sample for analysis. As shown in Table 1, we can see that probe was able to determine the concentration of spiked HSO_3^- and SO_3^{2-} in these real food samples with good recovery ranging from 97.5% to 102.6% and 97.4% to 104.0% respectively, indicating that this probe could potentially be used for quantitatively detecting bisulfite/sulfite in real food samples.

4. Conclusion

In summary, we have synthesized a colorimetric probe for the detection of bisulfite/sulfite anions, that works based on the Michael addition of anions to α, β-unsaturated ketones. The basic and nonpolar microenvironment provided by cationic surfactant CTAB enables the easy occurrence of the reaction in an aqueous solution, which allows the detection of both of the analytes (HSO_3^- and SO_3^{2-}). The obtained results indicate that the probe could potentially be used in the selective recognition of bisulfite/sulfite in real food samples.

Conflicts of interest

There are no conflicts to declare.

Acknowledgements

The authors (SP) thank the University Grants Commission, Government of India for financial support. We appreciate Dr Jambu S, Mr Kalidass K, Mr Chindhu S, and Mr Ramshad K for their valuable suggestions.

References

1 A. Hansell and C. Oppenheimer, Health hazards from volcanic gases: a systematic literature review, *Arch. Environ. Health*, 2004, **59**, 628–639.
2 J. S. Pandey, R. Kumar and S. Devotta, Health risks of NO_2, SPM and SO_2 in Delhi (India), *Atmos. Environ.*, 2005, **39**, 6868–6874.
3 N. Sang, Y. Yun, H. Li, L. Hou, M. Han and G. Li, SO_2 inhalation contributes to the development and progression of ischemic stroke in the brain, *Toxicol. Sci.*, 2010, **114**, 226–236.
4 D. Liu, H. Jin, C. Tang and J. Du, Sulfur dioxide: a novel gaseous signal in the regulation of cardiovascular functions, *Mini-Rev. Med. Chem.*, 2010, **10**, 1039–1045.

5 Y. Yun, R. Gao, H. Yue, G. Li, N. Zhu and N. Sang, Synergistic effects of particulate matter (PM_{10}) and SO_2 on human non-small cell lung cancer A549 via ROS-mediated NF-κB activation, *J. Environ. Sci.*, 2015, **31**, 146–153.

6 W. Zhang, F. Huo, F. Cheng and C. Yin, Employing an ICT-FRET integration platform for the real-time tracking of SO_2 metabolism in cancer cells and tumor models, *J. Am. Chem. Soc.*, 2020, **142**, 6324–6331.

7 Z. Meng, G. Qin, B. Zhang and J. Bai, DNA damaging effects of sulfur dioxide derivatives in cells from various organs of mice, *Mutagenesis*, 2004, **19**, 465–468.

8 T. Fazio and C. R. Warner, A review of sulphites in foods: analytical methodology and reported findings, *Food Addit. Contam.*, 1990, **7**, 433–454.

9 S. L. Bahna and J. G. Burkhardt, *The dilemma of allergy to food additives*, Allergy & Asthma Proceedings, 2018.

10 Z. Zhong, G. Li, B. Zhu, Z. Luo, L. Huang and X. Wu, A rapid distillation method coupled with ion chromatography for the determination of total sulphur dioxide in foods, *Food Chem.*, 2012, **131**, 1044–1050.

11 D. Urupina, V. Gaudion, M. N. Romanias, M. Verriele and F. Thevenet, Method development and validation for the determination of sulfites and sulfates on the surface of mineral atmospheric samples using reverse-phase liquid chromatography, *Talanta*, 2020, **219**, 121318.

12 K. Xiang, S. Chang, J. Feng, C. Li, W. Ming, Z. Liu, *et al.*, A colorimetric and ratiometric fluorescence probe for rapid detection of SO_2 derivatives bisulfite and sulfite, *Dyes Pigm.*, 2016, **134**, 190–197.

13 G. Asaithambi and V. Periasamy, Ratiometric sensing of sulfite/bisulfite ions and its applications in food samples and living cells, *J. Photochem. Photobiol., A*, 2020, **389**, 112214.

14 C. Nandhini, P. S. Kumar, R. Shanmugapriya, K. Vennila, A. G. Al-Sehemi, M. Pannipara, *et al.*, A combination of experimental and TD-DFT investigations on the fluorescent detection of sulfite and bisulfite ions in aqueous solution via nucleophilic addition reaction, *J. Photochem. Photobiol., A*, 2022, **425**, 113668.

15 Y. Zhou, J. Gou, Y.-X. Zhou, C. Liu, X. Xiao and H.-J. Liu, Tunable energy level induced fluorescence enhancement in copper functionalized silicon quantum dots for highly selective detection of bisulfite, *Sens. Actuators, B*, 2022, **370**, 132444.

16 A. Isaac, A. J. Wain, R. G. Compton, C. Livingstone and J. Davis, A novel electroreduction strategy for the determination of sulfite, *Analyst*, 2005, **130**, 1343–1344.

17 P. Begum, T. Morozumi, T. Kawaguchi and T. Sone, Development of an Electrochemical Sensing System for Wine Component Analysis, *ACS Food Sci. Technol.*, 2021, **1**, 2030–2040.

18 J. M. Vahl and J. E. Converse, Ripper procedure for determining sulfur dioxide in wine: collaborative study, *J. Assoc. Off. Anal. Chem.*, 1980, **63**, 194–199.

19 L. Zhang, L. Wang, X. Zhang and Z.-J. Zhu, A colorimetric and fluorescent probe for sulfite/bisulfite based on conjugated benzothiazole derivative and imaging application in living cells, *J. Photochem. Photobiol., A*, 2020, **395**, 112498.

20 J. H. Han, W. Y. Gao, L. H. Feng, Y. Wang and S. M. Shuang, An AIE-active probe for selective fluorometric–colorimetric detection of HSO_3^- in aqueous solution and real samples, *J. Photochem. Photobiol., A*, 2021, **421**, 113515.

21 S. Roy, A. Maity, N. Mudi, M. Shyamal and A. Misra, Rhodamine scaffolds as real time chemosensors for selective detection of bisulfite in aqueous medium, *Photochem. Photobiol. Sci.*, 2019, **18**, 1342–1349.

22 D. Don, K. Velmurugan, J. Prabhu, N. Bhuvanesh, A. Thamilselvan and R. Nandhakumar, A dual analyte fluorescent chemosensor based on a furan-pyrene conjugate for Al^{3+} & HSO_3^-, *Spectrochim. Acta, Part A*, 2017, **174**, 62–69.

23 P. Hou, S. Chen, K. Voitchovsky and X. Song, A colorimetric and ratiometric fluorescent probe for sulfite based on an intramolecular cleavage mechanism, *Luminescence*, 2014, **29**, 749–753.

24 M. G. Choi, J. Hwang, S. Eor and S.-K. Chang, Chromogenic and fluorogenic signaling of sulfite by selective deprotection of resorufin levulinate, *Org. Lett.*, 2010, **12**, 5624–5627.

25 K. Wang, W. Wang, S.-Y. Chen, J.-C. Guo, J.-H. Li, Y.-S. Yang, *et al.*, A novel Near-Infrared rhodamine-derivated turn-on fluorescence probe for sensing SO_3^{2-} detection and their bio-imaging in vitro and in vivo, *Dyes Pigm.*, 2021, **188**, 109229.

26 A. V. Leontiev and D. M. Rudkevich, Revisiting noncovalent SO_2^- amine chemistry: an indicator − displacement assay for colorimetric detection of SO_2, *J. Am. Chem. Soc.*, 2005, **127**, 14126–14127.

27 Y. Sun, C. Zhong, R. Gong, H. Mu and E. Fu, A ratiometric fluorescent chemodosimeter with selective recognition for sulfite in aqueous solution, *J. Org. Chem.*, 2009, **74**, 7943–7946.

28 Y. Yang, F. Huo, J. Zhang, Z. Xie, J. Chao, C. Yin, *et al.*, A novel coumarin-based fluorescent probe for selective detection of bissulfite anions in water and sugar samples, *Sens. Actuators, B*, 2012, **166**, 665–670.

29 X.-F. Yang, M. Zhao and G. Wang, A rhodamine-based fluorescent probe selective for bisulfite anion in aqueous ethanol media, *Sens. Actuators, B*, 2011, **152**, 8–13.

30 M. Albrecht, R. A. Gossage, M. Lutz, A. L. Spek and G. van Koten, Diagnostic organometallic and metallodendritic materials for SO_2 gas detection: reversible binding of sulfur dioxide to arylplatinum (II) complexes, *Chem.–Eur. J.*, 2000, **6**, 1431–1445.

31 J. Chao, X. Wang, Y. Liu, Y. Zhang, F. Huo, C. Yin, *et al.*, A pyrene-thiophene based fluorescent probe for ratiometric sensing of bisulfite and its application in vivo imaging, *Sens. Actuators, B*, 2018, **272**, 195–202.

32 X. Dai, T. Zhang, Z.-F. Du, X.-J. Cao, M.-Y. Chen, S.-W. Hu, *et al.*, An effective colorimetric and ratiometric fluorescent probe for bisulfite in aqueous solution, *Anal. Chim. Acta*, 2015, **888**, 138–145.

33 H. Feng, J. Liu, A. Qaitoon, Q. Meng, Y. Sultanbawa, Z. Zhang, *et al.*, Responsive small-molecule luminescence

probes for sulfite/bisulfite detection in food samples, *TrAC, Trends Anal. Chem.*, 2021, **136**, 116199.

34 T. Li, X. Chen, K. Wang and Z. Hu, Small-Molecule Fluorescent Probe for Detection of Sulfite, *Pharmaceuticals*, 2022, **15**, 1326.

35 Y. Sun, D. Zhao, S. Fan, L. Duan and R. Li, Ratiometric fluorescent probe for rapid detection of bisulfite through 1, 4-addition reaction in aqueous solution, *J. Agric. Food Chem.*, 2014, **62**, 3405–3409.

36 Y. Sun, S. Fan, S. Zhang, D. Zhao, L. Duan and R. Li, A fluorescent turn-on probe based on benzo [e] indolium for bisulfite through 1, 4-addition reaction, *Sens. Actuators, B*, 2014, **193**, 173–177.

37 M.-Y. Wu, K. Li, C.-Y. Li, J.-T. Hou and X.-Q. Yu, A water-soluble near-infrared probe for colorimetric and ratiometric sensing of SO_2 derivatives in living cells, *Chem. Commun.*, 2014, **50**, 183–185.

38 H. Tian, J. Qian, Q. Sun, H. Bai and W. Zhang, Colorimetric and ratiometric fluorescent detection of sulfite in water via cationic surfactant-promoted addition of sulfite to α, β-unsaturated ketone, *Anal. Chim. Acta*, 2013, **788**, 165–170.

39 H.-W. Chen, H.-C. Xia, O. Hakeim and Q.-H. Song, Phenothiazine and semi-cyanine based colorimetric and fluorescent probes for detection of sulfites in solutions and in living cells, *RSC Adv.*, 2021, **11**, 34643–34651.

40 M. Gómez, E. G. Perez, V. Arancibia, C. Iribarren, C. Bravo-Díaz, O. García-Beltrán, *et al.*, New fluorescent turn-off probes for highly sensitive and selective detection of SO_2 derivatives in a micellar media, *Sens. Actuators, B*, 2017, **238**, 578–587.

41 M. Gómez, M. E. Aliaga, V. Arancibia, A. Moya, C. Segura, M. T. Nunez, *et al.*, Detection of SO_2 derivatives using a new chalco-coumarin derivative in cationic micellar media: application to real samples, *RSC Adv.*, 2018, **8**, 31261–31266.

42 B. Rajashekar, P. Sowmendran, S. S. S. Sai and G. N. Rao, Synthesis, characterization and two-photon absorption based broadband optical limiting in diarylideneacetone derivative, *J. Photochem. Photobiol., A*, 2012, **238**, 20–23.

43 R. Badugu, J. R. Lakowicz and C. D. Geddes, Enhanced fluorescence cyanide detection at physiologically lethal levels: reduced ICT-based signal transduction, *J. Am. Chem. Soc.*, 2005, **127**, 3635–3641.

44 M. L. Satnami, S. Dhritlahre, R. Nagwanshi, I. Karbhal, K. K. Ghosh and F. Nome, Nucleophilic Attack of Salicylhydroxamate Ion at C═O and P═O Centers in Cationic Micellar Media, *J. Phys. Chem. B*, 2010, **114**, 16759–16765.

45 C. A. Bunton, M. M. Mhala and J. R. Moffatt, Nucleophilic reactions in zwitterionic micelles of amine oxide or betaine sulfonate surfactants, *J. Phys. Chem.*, 1989, **93**, 854–858.